Journal of Applied Pharmaceutical Research
Volume 14 Issue 2, Year of Publication 2026, Page 128 – 139
DOI: https://doi.org/10.69857/joapr.v14i2.1923

Check for updates

Research Article

JOURNAL OF APPLIED PHARMACEUTICAL RESEARCH | JOAPR
www.japtronline.com *ISSN: 2348 – 0335*

EXTRACTION AND PHYSICOCHEMICAL–THERMAL CHARACTERIZATION OF LEAF MUCILAGE FROM BUTEA MONOSPERMA WITH POTENTIAL RELEVANCE TO BIODEGRADABLE MATERIALS

Aastha Sharma, Meenakshi Bajpai, Anuj Garg*

Article Information
Received: 28th September 2025
Revised: 15th December 2025
Accepted: 3rd February 2026
Published: 15th March 2026

Keywords
Butea monosperma, mucilage, physicochemical characterization, thermal analysis, polysaccharides, biodegradable materials.

ABSTRACT
Background: Growing concerns over the persistence of petroleum-based plastics have renewed interest in plant-derived polysaccharides as sustainable material precursors. **Methodology:** In this work, mucilage extracted from *Butea monosperma* leaves was examined using comprehensive physicochemical, rheological, thermal, morphological, and solid-state characterisation to assess its properties. **Result and Discussion:** The extraction process yielded 10.58±0.42% (n=3) mucilage. Powder flow analysis indicated acceptable handling characteristics, with an angle of repose of 29.17±1.34°, Carr's index of 17.18±1.02%, and a Hausner ratio of 1.20±0.04. Aqueous dispersions (1.5% w/v) displayed shear-dependent viscosity over the range of 10–150 rpm, consistent with pseudoplastic flow behaviour. Dynamic light scattering measurements showed a mean hydrodynamic diameter of approximately 1085 nm, while the zeta potential value of –11.6 mV suggested moderate electrostatic stability of the dispersion. FTIR spectra confirmed the polysaccharide nature of the mucilage through characteristic hydroxyl, aliphatic, carbonyl, and glycosidic bands. X-ray diffraction revealed a predominantly amorphous structure with limited semi-crystalline domains. Thermal analysis showed minor mass loss below 190°C, followed by a principal degradation stage between 226 and 322 °C with an overall mass loss of ~61.9%, while DSC analysis identified multiple endothermic transitions, including a major event at 275.99°C. **Conclusion:** Collectively, these findings establish reproducible yield, non-Newtonian rheology, moderate thermal stability, and an amorphous solid-state profile for *Butea monosperma* leaf mucilage. The observed properties suggest their potential relevance as a plant-based biopolymer and merit further investigation through material fabrication, mechanical and barrier testing, biodegradation assessment, and safety evaluation.

INTRODUCTION

Plastic waste has evolved into one of the most challenging environmental burdens of the modern era, largely because conventional plastics resist degradation and persist in natural ecosystems for decades [1]. Their accumulation has been strongly associated with land and water pollution, and the

*Institute of Pharmaceutical Research, G.L.A. University, Mathura-281406, Uttar Pradesh, India.

***For Correspondence:** **anuj.garg@gla.ac.in**

consequences extend far beyond visible litter [2]. Concerns have grown not only because of their environmental footprint but also due to the possibility of chemical leaching, which may compromise food and water quality. Together, these issues have intensified the search for alternative materials that can perform the protective functions of plastics without contributing to long-term ecological harm [3]. Growing recognition of the ecological burden of petroleum-based plastics has intensified interest in biopolymers derived from renewable, natural sources. These materials have gained traction because they degrade more readily in the environment and typically exhibit a far smaller ecological footprint [4]. Over the past decade, numerous plant- and animal-based macromolecules- such as starches, cellulosic fibres, gums, mucilage, gelatin, and alginates—have been explored for their potential to generate functional packaging materials [5]. Their growing adoption also reflects shifting consumer expectations toward safer, minimally processed, and environmentally responsible packaging options [6]. On the industrial front, improvements in extraction and purification methods, along with advances in blending and material-forming technologies, have made it increasingly feasible to substitute conventional plastics with biodegradable counterparts [7]. Compared with earlier characterisation studies on *Butea monosperma* mucilage, including our previous report [6] that primarily addressed extraction yield and basic physicochemical properties, the present study extends the analysis to include shear-dependent rheological behaviour, detailed thermal transitions (DSC onset, peak and endset), thermal degradation profile (TGA), zeta potential–based dispersion stability, particle size distribution, and solid-state structural features (XRD).

These additional parameters provide application-oriented insights into processability and thermal stability, rather than directly demonstrating material formation. Accordingly, the objectives of this work are: (i) to extract and quantify the yield of mucilage from *Butea monosperma* leaves under defined conditions, (ii) to systematically characterise its physico-chemical, micromeritic, rheological, thermal, morphological, and solid-state properties, and (iii) to compare these properties with literature-reported mucilages commonly explored for biodegradable material applications. Measurements were performed in triplicate (n = 3). Among the various plant sources being explored for mucilage, such as Taro, Acacia, and many more, *Butea* monosperma, a deciduous tree native to the Indian subcontinent, stands out for its potential. Commonly referred to as the flame of the forest, this tree is found extensively throughout India, Bangladesh, and parts of Southeast Asia. Unlike our earlier work on *Butea monosperma* leaf mucilage, which focused primarily on basic physicochemical and FTIR characterisation [6], the present study extends the analysis to include rheological behaviour, zeta potential, particle-size distribution, XRD-based solid-state features, and detailed thermal transitions (TGA/DSC), providing parameters directly relevant to material processability [8].

Accordingly, the present study aims to extend prior characterisation by addressing the following specific objectives: (i) to extract and quantify the yield of mucilage from mature *Butea monosperma* leaves under defined conditions, (ii) to comprehensively characterise its physicochemical, micromeritic, rheological, thermal, morphological, and solid-state properties relevant to polymer processing, and (iii) to contextualise these properties through comparison with other commonly reported plant mucilages used in biodegradable material research. The study does not involve preparation or testing of actual materials; therefore, all application-related interpretations are presented as inferred potential based on material properties and existing literature. With global demand for eco-friendly packaging solutions on the rise and growing concerns about plastic waste, the exploration of plant-based alternatives such as Butea monosperma mucilage presents a viable and sustainable path forward. Harnessing such naturally abundant resources may offer an economic means of developing biodegradable plastics that can decompose safely, helping to mitigate the environmental burden of conventional plastics. To our knowledge, this is the first report consolidating rheological, electrokinetic, thermal, and solid-state parameters of *Butea monosperma* leaf mucilage in a single study.

MATERIALS AND METHODS

Materials

Leaves of *Butea monosperma* were collected from the campus of GLA University, Mathura, U.P., India, and authenticated by Prof. M. Badruzzaman Siddiqui, Department of Botany, Aligarh Muslim University.

Isolation of Mucilage

Fresh young leaves of *Butea monosperma* were gathered from trees during the summer season. The leaves were thoroughly washed and dried under controlled conditions. Dried leaves were ground to a very fine powder in a mechanical grinder. Powder was soaked (homogenised) in water for 2-3 hours. After soaking,

the slurry was held at 70 °C for 15-20 minutes to release mucilage from the leaves into the water, then left undisturbed for about an hour. Subsequently, the mixture was filtered through eight folds of muslin cloth to separate the marc and the solution, after which acetone in a 1:3 ratio (v/v) to the filtrate volume was added to precipitate the mucilage for about an hour [9]. The mucilage was filtered, oven-dried at a temperature not exceeding 50°C, collected, milled, and passed through an 80-mesh sieve. The finely powdered mucilage was kept in a desiccator for applications as shown in Figure 1 [10]. No further chemical purification of the extracted mucilage was performed prior to physicochemical and instrumental characterisation.

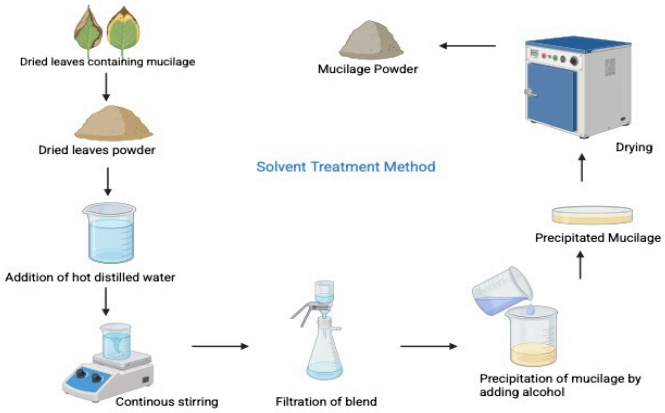

Figure 1: General method of mucilage extraction

CHARACTERISATION OF EXTRACTED MUCILAGE TECHNIQUES

To understand the properties of the extracted mucilage, the following characterisation techniques were employed:

Preliminary Confirmatory Tests for Mucilage: The occurrence of mucilage was confirmed through qualitative phytochemical screening employing Molisch's test as well as the ruthenium red staining method [11].

Determination of Percentage Yield: The percentage yield, an extraction efficiency, was quantified using the following equation [12]:

$$\%\ \boldsymbol{Yield} = \frac{\boldsymbol{weight\ of\ dried\ mucilage}}{\boldsymbol{Weight\ of\ starting\ plant\ material}} \times \mathbf{100}$$

Organoleptic Characterisation: The mucilage was subjected to tests for the organoleptic properties, i.e., colour, odour, taste, shape, texture & tactile sensation, using sensory organs as outlined in the correct procedure from the literature [13].

Solubility Assessment: Solubility behaviour of the extracted mucilage was assessed in a variety of solvents, including distilled water, methanol, ethanol, acetone, petroleum ether, and carbon tetrachloride [14].

Determination of Loss on Drying (LOD): Loss on drying was performed to quantify moisture and other volatile constituents in the mucilage. The mucilage powder was accurately weighed and placed in a previously dried and tared porcelain crucible. The sample was placed in the hot air oven maintained at 105 ± 2 °C until a constant weight was obtained. The percentage loss was then calculated from the variance between the initial and final weights [15]. [Corrected equations]

$$\boldsymbol{LOD}\ (\%) = \frac{\boldsymbol{W1 - W2}}{\boldsymbol{W1}} \times \mathbf{100}$$

Where, W1 = Initial weight of the sample before drying (in grams), W2 = Final weight of the sample after drying (in grams), 105 ± 2 °C.

Swelling Index (%): it can be determined by the formula:

$$\boldsymbol{Swelling\ Index}\ (\%) = \frac{\boldsymbol{Vt\ -\ V0}}{\boldsymbol{V0}} \times \mathbf{100}$$

Where V0 is the initial volume, Vt is the volume after swelling.

Micromeritics Evaluation: Bulk density, tapped density, Carr's index, Hausner's ratio, and angle of repose were determined using std. methods (n = 3).

Bulk Density (BD): The weight of the sample was measured and poured into a graduated cylinder. The volume was logged without tapping.

$$\boldsymbol{Bulk\ Density} = \frac{\boldsymbol{V}}{\boldsymbol{M}},$$

Where M = Mass of the sample, V = Volume of the sample

Tapped Density (TD): The cylinder containing the powder was tapped mechanically until a constant volume was obtained.

$$\boldsymbol{Tapped\ Density} = \frac{\boldsymbol{Vt}}{\boldsymbol{M}}$$

Where, M= Mass of the powder, Vt= Tapped volume

Carr's Index (Compressibility Index): Calculated utilising the formula:

$$\boldsymbol{Carr's\ Index} = \frac{\boldsymbol{TD - BD}}{\boldsymbol{TD}}$$

Hausner's Ratio: Calculated as the ratio of tapped to bulk density.

$$\boldsymbol{Hausner's\ Ratio} = \frac{\boldsymbol{TD}}{\boldsymbol{BD}}$$

Angle of Repose (θ): This is obtained with the powder allowed to flow through a funnel onto a flat surface, measuring the angle encompassed by the conical mass of powder in accordance with the formula given below:

$$\boldsymbol{tan(\theta)} = \frac{\boldsymbol{h}}{\boldsymbol{r}}$$

Where h is the height and r is the radius of the powder cone base [16].

Determination of Total Ash Content: The total ash content was determined to quantify the inorganic residue remaining after combustion, which may indicate the presence of extraneous matter. A known weight (2–3 g) of the mucilage powder was incinerated in a pre-weighed crucible using a muffle furnace set at 550 ± 25 °C until a light grey ash was gained. The crucible was chilled in a desiccator and weighed. The percentage of total ash was estimated based on the original weight of the sample [17].

pH Measurement: The pH of a 1% (w/v) aqueous solution of mucilage was determined using a calibrated digital pH meter under std. laboratory conditions [18].

Swelling Index: Specifically, 1 g of dried mucilage powder was positioned in a 100 mL stoppered graduated cylinder. After recording the initial volume, 1 mL of ethanol was added, followed by enough distilled water to bring the total volume to 100 mL. The mixture was shaken every 10 minutes during the first hour and allowed to stand undisturbed for 3 hours. This agitation-rest cycle was repeated every 3 hours, and the final volume was recorded after 24 hours. The procedure was carried out in triplicate, and the average value was reported [19].

$$\boldsymbol{Swelling\ Index}\ (\%) = \frac{\boldsymbol{Vt\ -\ V0}}{\boldsymbol{V0}} \times \boldsymbol{100}$$

Where V0 is the initial volume (ml), and Vt is the volume after 24 h (ml). Measurements were performed in triplicate.

Viscosity: The rheological behaviour of the extracted mucilage was assessed using a Brookfield rotational viscometer (DV1M). The mucilage solution was prepared at a concentration of 1.5% w/v by dispersing the dried mucilage powder in distilled water under constant stirring. The dispersion was allowed to hydrate completely overnight at ambient temperature and then filtered to remove insoluble residues. The final solution was equilibrated to 25 ± 0.5 °C before measurement. Viscosity measurements were carried out at varying rotational speeds (shear rates) ranging from 10 to 150 revolutions per minute (rpm) using Spindle No. 2, selected based on preliminary torque values to ensure readings remained within the optimal torque range (10%–90%). This spindle is commonly employed for medium-viscosity polysaccharide dispersions, providing accurate and stable readings across the tested rpm range [18].

Fourier Transform Infrared (FTIR) Spectroscopy: Using an FT-IR spectrometer (IRAffinity, Shimadzu, Japan), the mucilage's Fourier transform infrared spectroscopy (FTIR) spectra were analysed. After the mucilage was ground, combined with KBr, and placed in the sample holder, spectra ranging from 4000 to 400 cm-1 were acquired [20].

Scanning Electron Microscopy (SEM): A dried sample (mucilage) was sited using double-sided adhesive tape on a specifically made aluminium stub to conduct scanning electron microscopy. After a thin layer of gold was sputter-coated onto the stub, the stub was observed at 10 kV using a JSM 6100 scanning microscope (JEOL, Japan) [21].

Powder X-ray Diffraction (XRD): An X-ray diffractometer (X'Pert-PRO, Panalytical, UK) fitted with a copper tube and Cu K-alpha-1 radiation was used to determine the solid-state property of the isolated mucilage. The required sample quantity was examined, and scanning was carried out at 2=10 ° and 50 ° (specific length) with a scan step (time) of 29.84 s, while maintaining constant operating conditions of 45 kV of voltage, 40 mA of current, and 25 °C of temperature. On a glass slide measuring 3.5 cm by 2.5 cm and 0.2 cm thick, a uniform sample layer was placed on one side of a 2 g fine powder sample [22].

Thermogravimetric Analysis (TGA): Thermal properties of mucilage were determined using Thermogravimetric Analysis (Themys System thermal analyser, USA). After being weighed, a 20.6 mg mucilage sample was put on an uncovered 70 µL Alumina pan. The nitrogen flow rate was 60 mL/min. The sample was heated at 10 K/min from 30 to 1000°C [23].

Differential Scanning Calorimetry: Thermal analysis of the mucilage was performed using a Differential Scanning Calorimeter (Setline DSC, USA). A precisely weighed sample (6.182 mg) was sealed in an aluminium pan (40 µL) equipped with a pinhole lid. The analysis was conducted under a nitrogen atmosphere, maintaining a constant flow rate of 40 mL/min. The heating protocol involved an initial ramp from 25°C to 300°C at

a rate of -10 K/min, followed by a cooling cycle from 300°C to 25°C at the same rate. The DSC was carried out at SAIF, Punjab University in Chandigarh, India [24].

Zeta Potential: The zeta potential (ζ) of the extracted mucilage was determined using a Litesizer 500 Zetasizer (UK). For the analysis, a known quantity of the mucilage sample was accurately weighed and subsequently dispersed in 1.0 M sodium chloride solution at a concentration of 1.0 mg/mL. The mixture was then further diluted with deionised water & transferred into a DTS1070 disposable zeta cell cuvette. Measurements were carried out at 25°C, with a recorded count rate of 111.5 kilo counts per second (kcps) [25]. Measurements were performed in triplicate (n = 3).

Particle size analysis: A Zetasizer Litesizer 500, UK, was used to measure the particle size of the mucilage sample. The sample holder was filled with roughly 3.0 mL of sample dispersion. A 1.0 mg/mL dispersed sample was made in deionised water and placed in a cuvette to measure particle size. The count rate was 225.4 (kcps) at 25ºC. Dynamic Light Scattering, or DLS, is used to measure particle size. Particle size distribution is assessed using the velocity distribution of suspended particles in a dispersion medium. While an electric field is applied, the motion of particles is also studied. The research was carried out at SAIF, Punjab University in Chandigarh, India [26]. Measurements were conducted in triplicate (n = 3). Elemental composition was determined using CHNS analysis. Unless otherwise stated, all quantitative measurements were performed in triplicate (n = 3).

RESULTS AND DISCUSSION

Yield, Morphological, and Physicochemical Properties of Extracted Mucilage

The mucilage extraction yielded a substantial amount of material (10.58 ± 0.42%), demonstrating that *Butea monosperma* leaves are an excellent source of mucilage [17]. The mucilage had a smooth, transparent-to-pale-green appearance, and its gel-like consistency suggests it is rich in polysaccharides. Upon drying, the mucilage formed a flexible, soft powder. These properties are consistent with those reported for plant-derived polysaccharides investigated as biodegradable and other eco-friendly materials, as discussed in Table 1 and reported in the literature [28-31].

Table 1: Organoleptic Properties of Isolated Mucilage

Property	Description
Colour	Greenish-brown powder
Odour	Characteristic
Appearance	Lustrous
Identification	
Mounted in 96% ethanol	Clear angular masses.
Mounted in ruthenium red	Particles stained red
Mounted in iodine solution	Blue-stained particles

The physicochemical properties of the extracted mucilage were evaluated for suitability in biodegradable material production.

Micromeritics

The micromeritic characteristics of the extracted mucilage powder are crucial for understanding its suitability for use in the formulations. The results obtained for the flow, packing, and compaction properties of the mucilage powder are presented in Table 3. Based on the measured physicochemical and thermal characteristics, the mucilage shows potential relevance as a biopolymeric material. Any application-oriented implications remain inferred and require further experimental validation.

Viscosity

The viscosity of *Butea monosperma* mucilage dispersion (1.5% w/v) decreased progressively with increasing rotational speed between 10 and 150 rpm, demonstrating non-Newtonian, pseudoplastic behaviour. The apparent decrease in viscosity with increasing shear rate is attributed to alignment and partial disentanglement of polysaccharide chains under applied stress, reducing intermolecular resistance to flow. Measurements were conducted at 25±0.5 °C using a Brookfield rotational viscometer under the conditions described in the Methods section. Although model fitting was not performed, the monotonic decrease in viscosity with shear rate is characteristic of pseudoplastic polysaccharide dispersions. The viscosity is shown in Figure 2.

Table 2: Micromeritic Properties of Isolated Mucilage

Parameter	Result (Mean ± SD)	Key Indications
Angle of repose (θ)	29.17 ± 1.34	indicating acceptable to good flow characteristics
Tapped density (g/cm³)	0.64 ± 0.04	indicating acceptable to good flow characteristics
Bulk density (g/cm³)	0.53 ± 0.06	indicating acceptable to good flow characteristics
Compressibility index (%)	17.18 ± 1.02	indicating acceptable to good flow characteristics
Hausner's ratio	1.20 ± 0.04	indicating acceptable to good flow characteristics

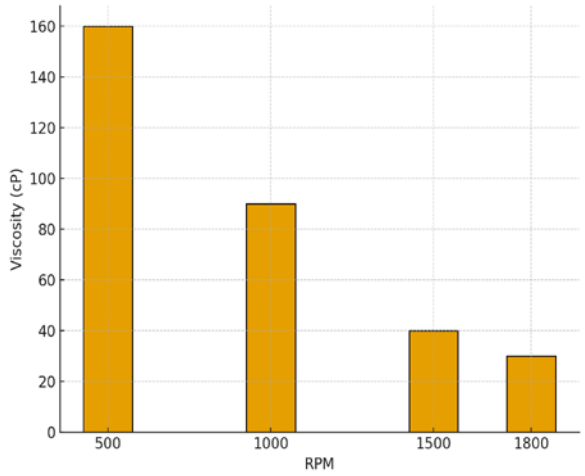

Figure 2: Flow properties of isolated mucilage

FTIR Spectroscopic Analysis

The FTIR spectrum of the mucilage, as shown in Figure 3, exhibited a broad band around 3319 cm^-1, conforming to the O-H stretching vibrations of hydroxyl groups. This suggests that the mucilage has hydrophilic properties, contributing to its ability to retain moisture, a desirable trait for biodegradable materials [8]. Additional peaks observed at 1746 cm^-1 and 1228 cm^-1 were attributed to C=O and C-O-C stretching vibrations, respectively, confirming the presence of polysaccharides in the mucilage [33].

The FTIR spectrum of the extracted mucilage, as shown in Figure 3, reveals significant absorption bands that indicate the occurrence of numerous functional groups associated with polysaccharides, confirming its polysaccharide nature and structural features commonly reported in biodegradable material research, as shown in Table 3 and reported in various literature. These functional groups confirm the structural integrity of the mucilage as a naturally derived biopolymer, capable of intermolecular hydrogen bonding, a structural feature frequently discussed in polysaccharide-based systems reported in the literature [34].

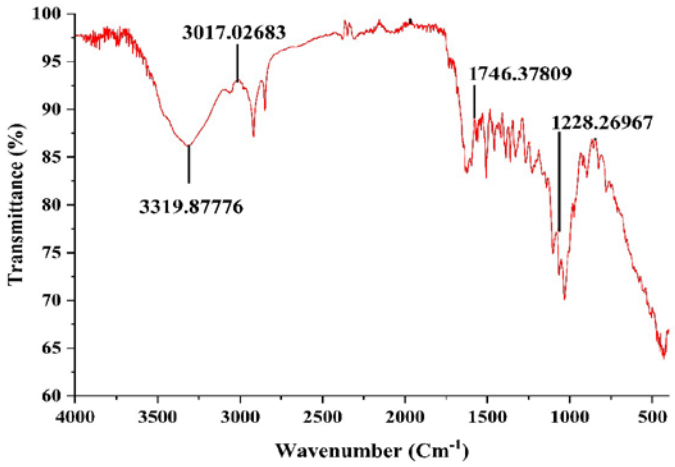

Figure 3: FTIR spectrum of isolated mucilage.

Table 3: FTIR of Isolated Mucilage

S.No	Wavenumber (cm^{-1})	Reference Wavenumber	Assigned for	Observation
1	3319	3600–3200	O–H stretch	Confirms the hydrophilic nature
2	3017	3000–2850	C–H stretch	Contributes to flexibility
3	1746	1750–1680	C=O stretch	commonly associated with polysaccharide networks reported in film-forming systems, as reported in the literature.
4	1228	1300–1000	C–O–C	Indicates glycosidic bonds

Comparison with Other Mucilages

To contextualise the spectral characteristics, the obtained FTIR profile is compared with mucilages from other plant sources commonly employed in biodegradable material production, as shown in Table 4, such as Okra (*Abelmoschus esculentus*), Plantago (*Plantago ovata*), and Basil seed (*Ocimum basilicum*) mucilages [35-37]. The functional attributes are likely to contribute positively to the functional attributes reported for polysaccharide-based systems in the literature, warranting further investigation into their performance in composite or crosslinked formulations, as supported by the literature [38].

Table 4: Comparison of FTIR Parameters from Different Mucilage Sources

Functional Group	*Butea Monosperma*	Okra	*Plantago ovata*	Basil Seed
O–H stretch (~3300 cm^{-1})	Strong, broad	Strong, broad	Strong, broad	Strong, broad
C–H stretch (~3000 cm^{-1})	Present (3017 cm^{-1})	Present (~2920 cm^{-1})	Often absent or weak	Weak or absent
C=O stretch (~1746 cm^{-1})	Sharp, distinct	Broad or weak	Present but less intense	Present
C–O–C / glycosidic bond	Prominent (~1228 cm^{-1})	Present (~1020–1150 cm^{-1})	Present (~1050–1150 cm^{-1})	Present (~1040–1160 cm^{-1})

Scanning electron microscopy

SEM images provide qualitative information on surface morphology and the dimensions of dried mucilage agglomerates (average feature size ~46 µm). In contrast, dynamic light scattering measures the hydrodynamic diameter of dispersed entities in aqueous suspension (~1085 nm). These techniques probe different physical states of the material (dry vs hydrated), and the apparent size discrepancy reflects aggregation and hydration effects rather than measurement inconsistencies.

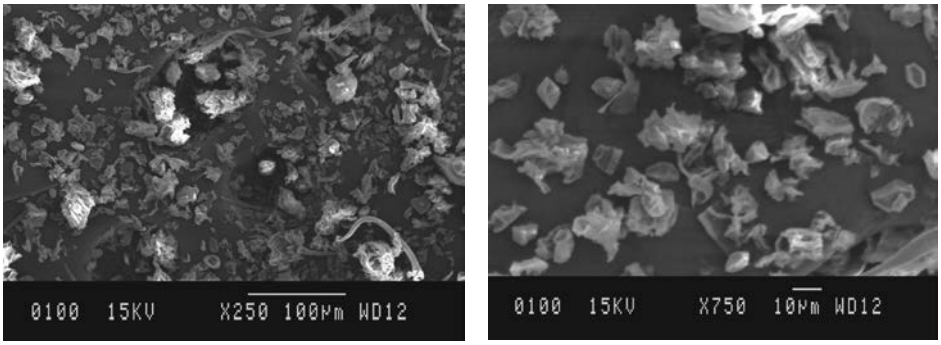

Figure 4: SEM micrographs of mucilage at scales (a) 250 µm and (b) 750 µm.

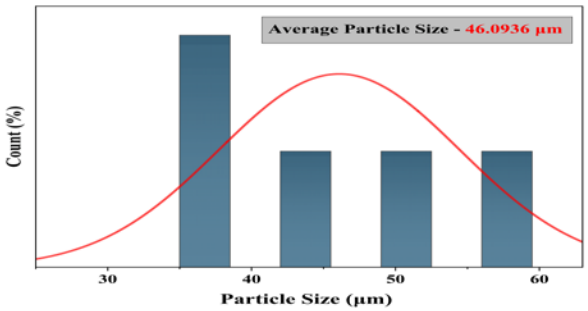

Figure 5: Average particle size as per SEM images. Measurements were conducted in triplicate (n = 3).

Powder X-ray Diffraction Analysis

The X-ray diffractogram of the mucilage powder shows a large peak with a maximum area at 2Θ=27.80, as shown in Figure 6. The average grain length is calculated as d-spacing = 3.20 Å, and the XRD pattern shows a broad diffraction peak, indicating an amorphous structure. This lack of crystallinity is commonly associated with flexibility in polysaccharide-based systems reported in the literature [40]. The diffractogram reveals a predominantly broad, diffuse scattering profile with a prominent peak at around 28° (2θ), suggesting the presence of both amorphous and semi-crystalline regions. The wide halo spanning 10°–25° (2θ) is typical of amorphous polysaccharides, indicating a lack of long-range molecular ordering, a desirable trait for biodegradable materials due to their enhanced flexibility and solubility [41]. The sharp diffraction peak at approximately 28° likely indicates localised crystallinity, possibly arising from residual inorganic salts or partial alignment of polysaccharide chains during mucilage drying. The smaller peaks across the diffractogram suggest semi-crystalline domains, attributed to densely packed polymer segments or interactions between the mucilage components and other entrapped molecules [42]. The coexistence of amorphous and semi-crystalline domains is frequently discussed in the literature as influencing the balance between structural integrity and flexibility in polysaccharide systems [43-47].

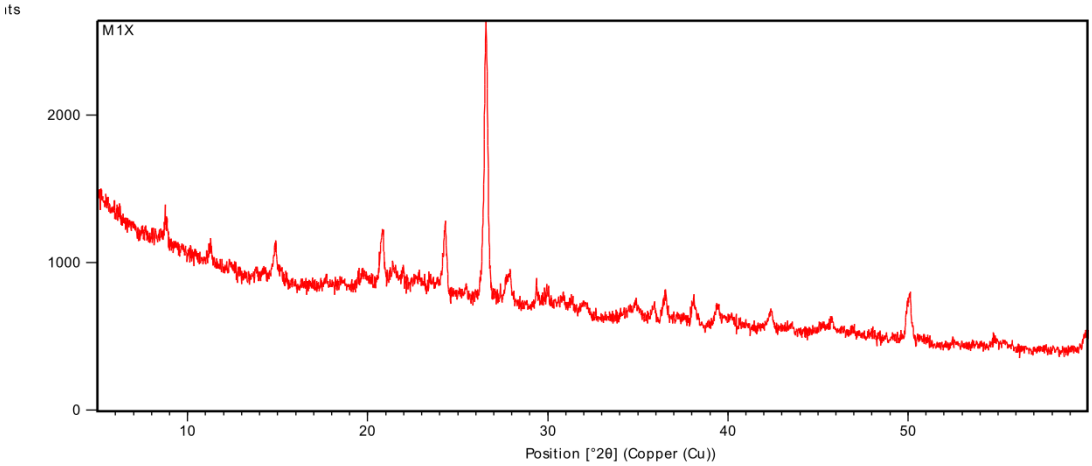

Figure 6: PXRD pattern of mucilage

Thermogravimetry Analysis and Stability

The thermal stability of the mucilage was evaluated using TGA, which revealed minimal weight loss (approx. 13%) up to 190ºC, as shown in Figure 7, indicating the presence of water. The subsequent weight loss occurs at around 290ºC. The thermal behaviour and stability statistics for gum are based on primary and derivative thermograms. The commencement of weight loss may be due to oxidation or polymer breakdown, indicating moderate thermal stability of the isolated mucilage. Thermogravimetric analysis (TGA) was employed to investigate and compare the thermal degradation behaviour of isolated mucilage. The TGA curve of the present study shows a clear thermal degradation profile, with the major decomposition occurring between 226.02°C & 322.01°C & a maximum degradation rate at 280.03°C. The material exhibited a total mass loss of 61.91% during the primary degradation phase, suggesting substantial breakdown of the mucilage matrix. The residual mass (~38%) indicates the presence of stable carbonaceous or inorganic remnants after pyrolysis [48]. All thermal analyses were performed on isolated mucilage powder, not films.

Differential scanning calorimetry

Thermal properties of biopolymers are critical for determining their applicability in packaging and other heat-sensitive environments. In this study, Differential Scanning Calorimetry (DSC) was employed to assess the thermal behaviour of the isolated mucilage. The DSC thermogram revealed three distinct endothermic events, indicative of a multiphase structural composition. As shown in Figure 8, the first thermal transition occurred at a peak temp. of 203.67°C, with an onset at 128.83°C and an endset at 230.15°C, representing a probable glass transition or melting of low-molecular-weight polysaccharide fractions. This transition suggests a moderate-to-strong polymeric network, capable of resisting early thermal deformation.

The second major endothermic peak at 275.99°C (onset at 231.40°C, endset at 331.24°C) is attributed to the melting or decomposition of semi-crystalline regions, signifying the principal thermal degradation phase. The third peak, occurring at 404.98°C, likely corresponds to the final decomposition or carbonisation of high-molecular-weight compounds such as cellulose or lignified residues. The respective enthalpy changes for these events were 35.54 J/g, 27.98 J/g, and 6.04 J/g [49].

Zeta Potential Analysis

Zeta potential measurements provide an indication of the surface charge and colloidal stability of mucilage in aqueous dispersions. The mucilage exhibited a zeta potential of –11.6 mV as shown in Figure 9, suggesting a moderately stable dispersion due to electrostatic repulsion between negatively charged particles. This is primarily attributed to the presence of acidic polysaccharides such as pectin or uronic acids. The negative charge enhances the mucilage's dispersibility & supports dispersion stability, which may be relevant for future formulation studies [49]. Measurements were performed in triplicate (n = 3).

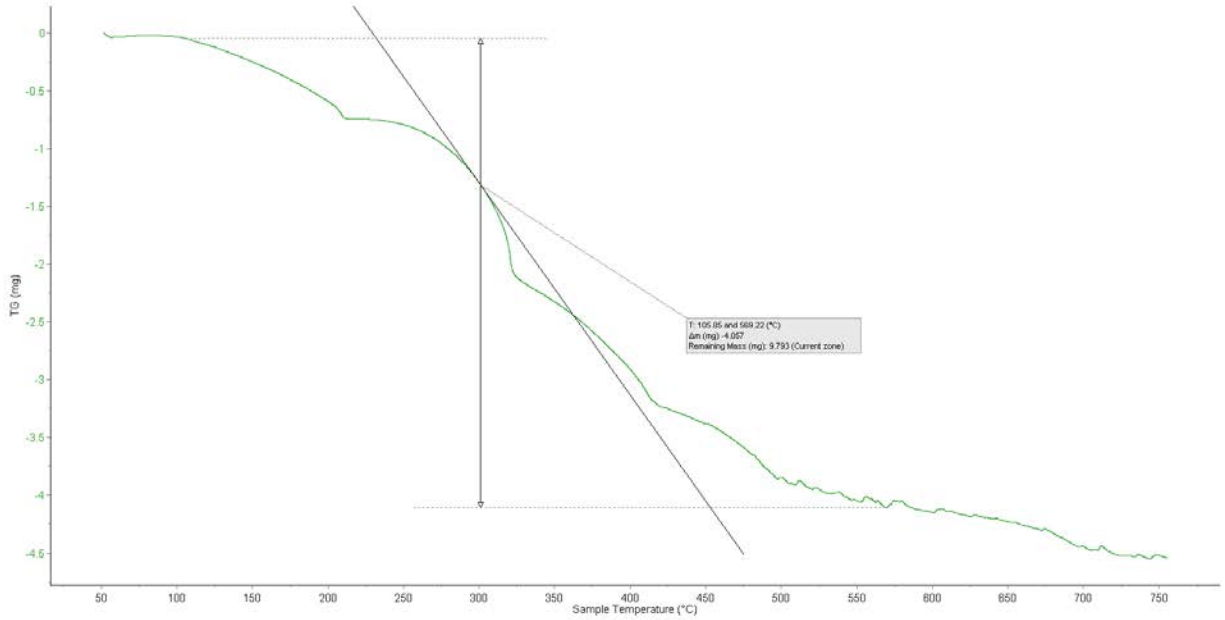

Figure 7: TGA thermogram of mucilage.

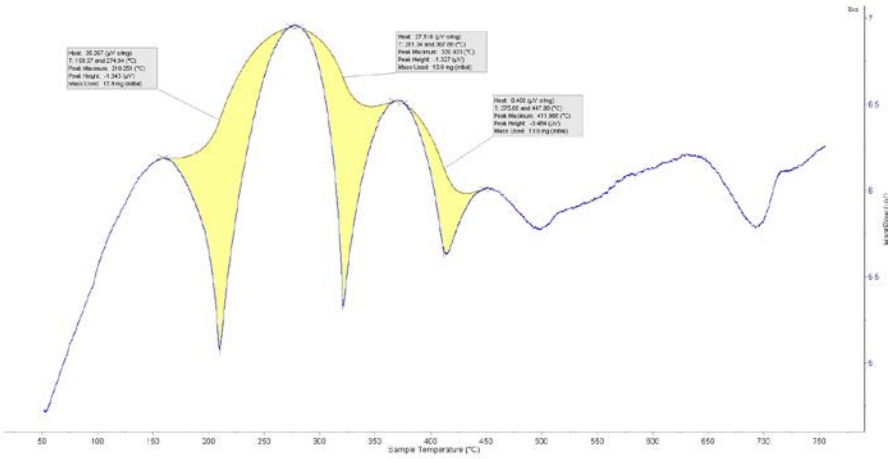

Figure 8: DSC thermogram of mucilage.

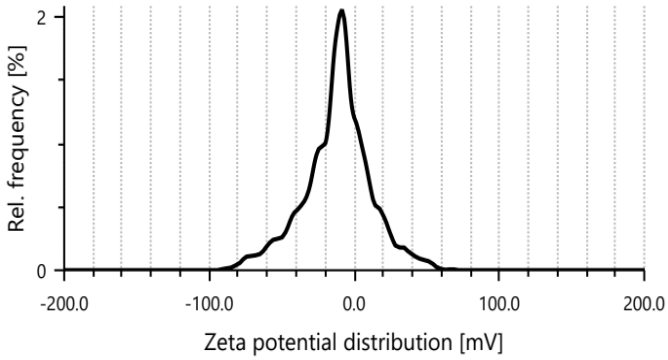

Figure 9: Zeta potential analysis of mucilage.

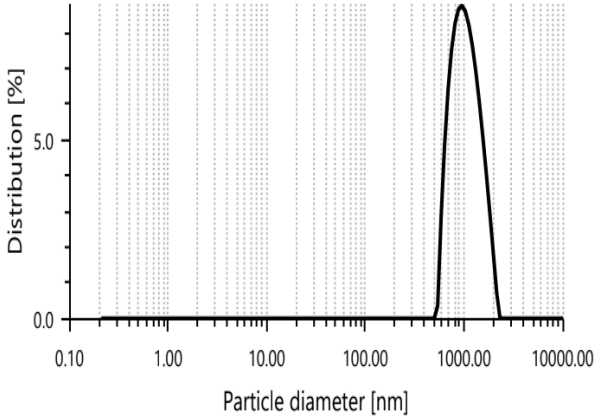

Figure 10: Particle size distribution of mucilage.

Particle Size Analysis

Particle size distribution was evaluated by means of dynamic light scattering (DLS). The mucilage particles in aqueous dispersion had an average hydrodynamic diameter of 1085 nm, as shown in Figure 10, with a polydispersity index (PDI) of 12%, indicating moderate uniformity in size distribution. This nanoscale particle size suggests potential relevance to dispersion-based applications reported in the literature, subject to further validation given its high surface area and material processability [50]. Measurements were conducted in triplicate (n = 3).

Elemental Composition (CHNS-O Analysis)

Elemental analysis of the mucilage was performed to determine its basic chemical makeup, as discussed in Table 5 and Figures 11a and b. The high oxygen and carbon content aligns with the presence of carbohydrate-rich polymers, while the small amounts of nitrogen and sulphur suggest trace proteins or other minor constituents. This composition reinforces the plant-derived polysaccharide nature of the mucilage and its suitability for bio-based polymer applications.

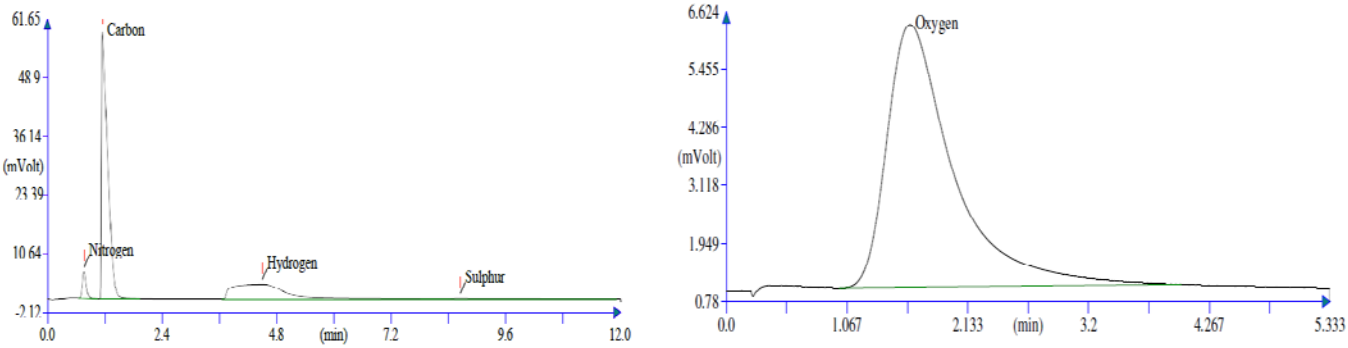

Figure 11: Elemental composition (CHNS-O) of mucilage.

Table 5: Elemental Composition of Isolated Mucilage

Element	Percentage Composition
Carbon (C)	26.122%
Hydrogen (H)	5.659%
Nitrogen (N)	2.496%
Sulfur (S)	0.808%
Oxygen (O)	35.960%

CONCLUSION

This study establishes that mucilage extracted from the leaves of *Butea monosperma* exhibits physicochemical, thermal, and morphological properties relevant to biodegradable material research. The material demonstrated good processability-related characteristics, pseudoplastic flow behaviour, and thermal stability up to approximately 200 °C. While the study confirms its potential as a renewable biopolymer, further investigations focusing on mechanical performance, biodegradation kinetics, and large-scale processing are required. In the current context of increasing plastic pollution and demand for sustainable materials, *Butea monosperma* mucilage may represent a promising plant-derived polysaccharide for further investigation in eco-friendly material research. Mucilages are plant-derived polymers that are affected by environmental and seasonal factors, which can impact their yield, quality, and production. The extraction and isolation of mucilage are complex processes. Mucilage yield, in addition to consistency, is affected by physical impairment to the plant element used for extraction, offering a significant challenge to prices and mass production capacity. Moisture content might contribute to microbial contamination during processing if not adequately stored. Isolating polysaccharides from protein-rich matrices needs efficient and selective pretreatment and extraction procedures. Understanding the structure-function link requires considering the mucilage's structure, chemical fingerprint, and biological function. Structure modification requires a combination of powerful analytical and sophisticated techniques.

The food and drug regulatory authorities must approve *Butea Monosperma* mucilage before being used commercially. Regulatory authorities require extensive stability and toxicity research before approving mucilage and related products. This study demonstrates that *Butea monosperma* leaf mucilage exhibits reproducible yield, polysaccharide-rich composition, pseudoplastic rheology, moderate thermal stability, and predominantly amorphous solid-state structure. These experimentally demonstrated properties indicate potential relevance for biodegradable material development. However, fabrication of materials, evaluation of mechanical and barrier properties, biodegradation, toxicity, and scalability studies are required before application or commercial claims can be substantiated.

ACKNOWLEDGEMENTS

The authors acknowledge SAIF, Panjab University, Chandigarh, for instrumental support.

FINANCIAL ASSISTANCE

NIL

CONFLICT OF INTEREST

The authors declare no conflict of interest.

AUTHOR CONTRIBUTION

Meenakshi Bajpai and Anuj Garg planned the study. Aastha Sharma performed the methodology, evaluation, data collection, and writing of this paper. All authors contributed to the drafting of the manuscript.

REFERENCES

[1] Kumar A, Meena R, Sharma A. Extraction and characterisation of mucilage from different plant sources: a review. *Int J Biol Macromol*, **149**, 640–8 (2020) https://doi.org/10.1016/j.ijbiomac.2020.01.164

[2] Venkatesan U, Muniyan R. Review on the extension of shelf life for fruits and vegetables using natural preservatives. *Food Sci Biotechnol*, **33(10)**, 2477–96 (2024) https://doi.org/10.1007/s10068-024-01602-3

[3] Rajput K, Kaur R, Thakur M. Functional properties and applications of bioplastics from plant-based mucilage. *Ind Crops Prod*, **188**, 115126 (2022) https://doi.org/10.1016/j.indcrop.2022.115126

[4] Thakur M, Singh D, Rajput K. Isolation and application of natural biopolymers for environmental sustainability. *Sustainable Dev*, **31**, 865–76 (2023) https://doi.org/10.1002/sd.2468

[5] Arshad MT, et al. Emerging trends in sustainable packaging of food products: an updated review. *J Nat Fibers*, **22(1)**, 114–32 (2025) https://doi.org/10.1080/15440478.2025.2505608

[6] Hossain M, Rahman M. Characterisation of mucilage extracted from *Butea monosperma* leaves: potential applications in bioplastics. *J Appl Polym Sci*, **137**, 48567 (2020) https://doi.org/10.1002/app.48567

[7] Kumar R, Singh A, Mehta M. Thermal stability and biodegradability of polysaccharides: insights from mucilage. *Polym Adv Technol*, **32**, 213–20 (2021) https://doi.org/10.1002/pat.5123

[8] Hussain S, Akhter R, Maktedar SS. Advancements in sustainable food packaging: from eco-friendly materials to innovative technologies. *Sustain Food Technol*, **2(5)**, 1297–1364 (2024) https://doi.org/10.1039/D4FB00021A

[9] Gamage A, Thiviya P, Liyanapathiranage A, Wasana MLD, Jayakodi Y, Bandara A, Manamperi A, Dassanayake RS, Evon P, Merah O, et al. Polysaccharide-based bioplastics: eco-friendly and sustainable solutions for packaging. *J Compos Sci*, **8**, 413 (2024) https://doi.org/10.3390/jcs8100413

[10] Silva RMP, Atanes SP, Fernandes SSF. Environmental impact of biodegradable packaging based on chia mucilage in real water bodies. *Processes*, **13**, 2381 (2025) https://doi.org/10.3390/pr13082381

[11] Mukaila YO, Adeyemi JO, Fawole OA. Towards sustainable biopolymer innovation: a review of *Opuntia ficus-indica* mucilage. *Processes*, **13**, 3837 (2025) https://doi.org/10.3390/pr13123837

[12] Alves RN, Cavalcanti MT, Pereira EM, Gomes JP, Silva WP, Gonçalves MC. Exploring cactus mucilage for sustainable food packaging: a bibliometric review. *Processes*, **13**, 1830 (2025) https://doi.org/10.3390/pr13061830

[13] El-Sayed HT, Salem AA, El-Sharaby AA. Mucilage-based composite films and coatings for food packaging applications: a review. *Int J Biol Macromol*, **300**, 140276 (2025) https://doi.org/10.1016/j.ijbiomac.2025.140276

[14] Huang Y, Yang J. Biodegradable composite films based on mucilage from *Opuntia ficus-indica*: functional and thermal properties. *Int J Biol Macromol*, **252**, 126456 (2023) https://doi.org/10.1016/j.ijbiomac.2023.126456

[15] Goyal R, Verma S, Vaish M, Shekhar A. Polysaccharide: a biodegradable biopolymer for edible films and coatings. *J Curr Res Food Sci*, **6**, 170–6 (2025) https://doi.org/10.1016/j.jcrfs.2025.170176

[16] Barros de Medeiros V, de Oliveira KAR, Queiroga TS, de Souza EL. Development and application of mucilage and bioactive compounds from Cactaceae to formulate novel and sustainable edible films and coatings to preserve fruits and vegetables: a review. *Foods*, **13(22)**, 3613 (2024) https://doi.org/10.3390/foods13223613

[17] Silva P, Nunes C, et al. Biodegradable packaging films based on plant polysaccharides: sustainability and functional properties. *Sustainable Chem*, **4(2)**, 215–32 (2023) https://doi.org/10.3390/suschem4020013

[18] Pastrana C, Teixeira JC, Valente F, et al. Biodegradable films from cactus mucilage and polyvinyl alcohol for food packaging applications. *Food Packag Shelf Life*, **35**, 101012 (2023) https://doi.org/10.1016/j.fpsl.2022.101012

[19] Ramírez-Ramírez JJ, Morán-Pineda I, et al. Physicochemical characterization of plant mucilage films for biodegradable packaging. *J Appl Polym Sci*, **141**, e55234 (2024) https://doi.org/10.1002/app.55234

[20] Liu Y, Wang X, Yang Y. Recent advances in edible and biodegradable films based on plant-derived polysaccharides. *Food Hydrocoll*, **137**, 108367 (2023) https://doi.org/10.1016/j.foodhyd.2022.108367

[21] Singh R, Kaur B, Singh S. Functional properties of natural plant polysaccharides for sustainable film formation. *Carbohydr Polym*, **315**, 120964 (2023) https://doi.org/10.1016/j.carbpol.2023.120964

[22] Yuen CB, et al. Natural polymer-based food packaging: paving the way to a greener future – a review. *Sustain Food Technol*, **3(4)**, 908–29 (2025) https://doi.org/10.1039/D5FB00021A

[23] Prasanna S, Verma P, Bodh S. The role of food industries in sustainability transition: a review. *Environ Dev Sustain*, **27(7)**, 15113–33 (2024) https://doi.org/10.1007/s10668-024-04642-1

[24] Martínez-Sanz M, Ruiz-Perez C, et al. Sustainable plant mucilage films in active packaging systems. *Food Packag Shelf Life*, **38**, 101125 (2024) https://doi.org/10.1016/j.fpsl.2023.101125

[25] Jahangiri F, Mohanty AK, Misra M. Sustainable biodegradable coatings for food packaging: challenges and opportunities. *Green Chem*, **26(9)**, 4934–74 (2024) https://doi.org/10.1039/D3GC02647G

[26] Oliveira AM, Machado R, dos Reis T. Biodegradable films from plant mucilage blends with starch and chitosan. *Int J Biol Macromol*, **310**, 141025 (2025) https://doi.org/10.1016/j.ijbiomac.2025.141025

[27] Dirpan A, et al. A review on biopolymer-based biodegradable film for food packaging: trends over the last decade and future research. *Polymers*, **15(13)**, 2781 (2023) https://doi.org/10.3390/polym15132781

[28] Rajan A, Ramana KV. Bio-based mucilage films: barrier and mechanical properties for food packaging. *J Clean Prod*, **418**, 140086 (2024) https://doi.org/10.1016/j.jclepro.2023.140086

[29] Panou A, Karabagias I. Biodegradable packaging materials for foods preservation: sources, advantages, limitations, and future perspectives. *Coatings*, **13(7)**, 1176 (2023) https://doi.org/10.3390/coatings13071176

[30] Motelica L, et al. Biodegradable antimicrobial food packaging: trends and perspectives. *Foods*, **9(10)**, 1438 (2020) https://doi.org/10.3390/foods9101438

[31] Kumar S, Rana V, et al. Biopolymer blend films from cactus mucilage and polyvinyl alcohol. *Polym Test*, **129**, 108433 (2025) https://doi.org/10.1016/j.polymertesting.2024.108433

[32] Versino F, et al. Sustainable and bio-based food packaging: a review on past and current design innovations. *Foods*, **12(5)**, 1057 (2023) https://doi.org/10.3390/foods12051057

[33] Pérez A, Gómez M, et al. Biofilms from natural polysaccharides and plasticizers: mechanical and barrier evaluation. *Int J Biol*

Macromol, **234**, 124115 (2023) https://doi.org/10.1016/j.ijbiomac.2023.124115

[34] Li R, Wang Y. Polysaccharide-chitosan films for biodegradable packaging materials. *Carbohydr Polym*, **319**, 121176 (2024) https://doi.org/10.1016/j.carbpol.2023.121176

[35] Silva P, Nunes C, et al. Plant mucilage-based hydrogels with antimicrobial activity for food protection. *Food Chem*, **437**, 137723 (2024) https://doi.org/10.1016/j.foodchem.2023.137723

[36] González A, Rodríguez F, et al. Sustainable films from plant mucilage: processing and environmental impact. *J Appl Polym Sci*, **142**, e56189 (2025) https://doi.org/10.1002/app.56189

[37] Patel M, Shah S, et al. Development of plant-derived composite biopolymers for food packaging applications. *J Biobased Mater Bioenergy*, **18**, 512–21 (2024) https://doi.org/10.1166/jbmb.2024.2342

[38] Ahmed J, Varshney N. Biopolymer films with enhanced water barrier and mechanical properties from plant mucilage. *Int J Biol Macromol*, **305**, 140711 (2025) https://doi.org/10.1016/j.ijbiomac.2025.140711

[39] Rajendran S, et al. Replacement of petroleum-based products with plant-based materials, green and sustainable energy—a review. *Eng Rep*, **7(4)**, e70108 (2025) https://doi.org/10.1002/eng2.70108

[40] Rabelo LS, et al. The future of sustainable packaging: exploring biodegradable solutions through extrusion and 3D printing. *Polymers*, **17(1)**, 25 (2025) https://doi.org/10.3390/polym17010025

[41] Yin Y, Woo MW. Transitioning of petroleum-based plastic food packaging to sustainable bio-based alternatives. *Sustain Food Technol*, **2(2)**, 412–35 (2024) https://doi.org/10.1039/D2FB00044C

[42] Hussain S, et al. Performance of biodegradable active packaging in the preservation of fresh-cut fruits. *Polymers*, **16(24)**, 3518 (2024) https://doi.org/10.3390/polym16243518

[43] Reichert CL, et al. Bio-based packaging: materials, modifications, industrial applications and sustainability. *Polymers*, **12(7)**, 1558 (2020) https://doi.org/10.3390/polym12071558

[44] Gamage A, Thiviya P, Liyanapathiranage A, et al. Polysaccharide-based bioplastics: eco-friendly and sustainable solutions for packaging. *J Compos Sci*, **8(10)**, 413 (2024) https://doi.org/10.3390/jcs8100413

[45] Silva RMP, Atanes SP, Fernandes SSF. Environmental impact of biodegradable packaging based on chia mucilage in real water bodies. *Processes*, **13(8)**, 2381 (2025) https://doi.org/10.3390/pr13082381

[46] Akafian S, Shekarchizadeh H. Development of hydrophobic composite films from ethylcellulose and lipids for packaging. *Int J Food Sci Technol*, **60(2)**, 442–56 (2025) https://doi.org/10.1111/ijfs.16854

[47] Arora S, Yadav M, et al. Natural polymer films from plant mucilage: biodegradability and sustainability assessments. *J Clean Prod*, **402**, 139998 (2024) https://doi.org/10.1016/j.jclepro.2023.139998

[48] Mukaila YO, Adeyemi JO, Fawole OA. Towards sustainable biopolymer innovation: a review of *Opuntia ficus-indica* mucilage. *Processes*, **13(12)**, 3837 (2025) https://doi.org/10.3390/pr13123837

[49] Jain P, Gupta D, Agarwal R. Future trends in bioplastics derived from plant mucilage. *J Clean Prod*, **245**, 118127 (2020) https://doi.org/10.1016/j.jclepro.2019.118127

[50] Tosif MM, et al. A comprehensive review on plant-derived mucilage: characterisation, functional properties, applications, and its utilisation for nanocarrier fabrication. *Polymers*, **13**, 1066 (2021) https://doi.org/10.3390/polym13071066